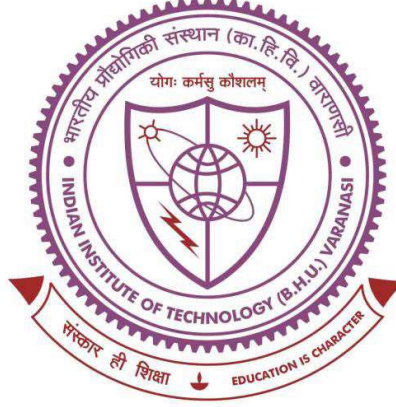


***HELICAL MODES AND POLARIZATION
GUIDING TO DELIVER OPTICAL INFORMATION
THROUGH RANDOM SCATTERER: LOOKING
THROUGH RANDOMNESS***



**A thesis submitted in partial fulfillment for the
Award of Degree
Doctor of Philosophy
in
Physics
by
*Tushar Sarkar***

**DEPARTMENT OF PHYSICS
INDIAN INSTITUTE OF TECHNOLOGY
(BANARAS HINDU UNIVERSITY)
VARANASI – 221005**

Roll Number: 18171502

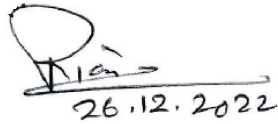
December, 2022

CERTIFICATE

It is certified that the work contained in the thesis titled “Helical modes and polarization guiding to deliver optical information through random scatterer: Looking through randomness” by Tushar Sarkar has been carried out under my supervision and that this work has not been submitted elsewhere for a degree.

It is further certified that the student has fulfilled all the requirements of the comprehensive examination, candidacy, and SOTA for the award of a Ph.D. Degree.

Signature:



26.12.2022

Supervisor

Dr. Rakesh Kumar Singh
(Associate Professor)
Department of Physics
Indian Institute of Technology
(Banaras Hindu University)
Varanasi-221005 (U.P), India

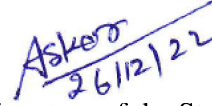
Associate Professor
Department of Physics
Indian Institute of Technology
(Banaras Hindu University)
Varanasi-221005

DECLARATION BY THE CANDIDATE

I, "*Tushar Sarkar*", certify that the work embodied in this thesis is my own bona fide work carried out by me under the supervision of "*Dr. Rakesh Kumar Singh*" from "*January 2019*" to "*December 2022*", at the "*DEPARTMENT OF PHYSICS*", Indian Institute of Technology (BHU), Varanasi. The matter embodied in this thesis has not been submitted for the award of any other degree/diploma. I declare that I have faithfully acknowledged and given credit to the research workers wherever their works have been cited in my work in this thesis. I further declare that I have not willfully copied any other's work, paragraphs, text, data, results, *etc.*, reported in journals, books, magazines, reports dissertations, thesis, *etc.*, or available on websites and have not included them in this thesis and have not cited as my work.

Date: **26 December 2022**


Place: **IIT (BHU), Varanasi**


Signature of the Student
(*Tushar Sarkar*)

CERTIFICATE BY THE SUPERVISOR

It is certified that the above statement made by the student is correct to the best of my knowledge.

Supervisor

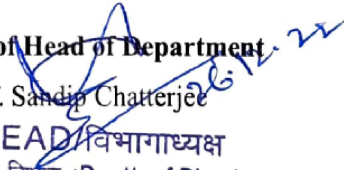

26.12.2022

Dr. Rakseh Kumar Singh
(Associate Professor)

Associate Professor
Department of Physics
Indian Institute of Technology
(Banaras Hindu University)
Varanasi-221005

Signature of Head of Department

Prof. Sandip Chatterjee


HEAD/विभागाध्यक्ष
भौतिकी विभाग/Deptt. of Physics
भा०प्रौ०सं०/(का०हि०वि०)/IIT (BHU)
वाराणसी/Varanasi-221005

COPYRIGHT TRANSFER CERTIFICATE

Title of the Thesis: Helical modes and polarization guiding to deliver optical information through random scatterer: Looking through randomness

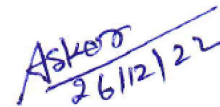
Name of the Student: Tushar Sarkar

Copyright Transfer

The undersigned hereby assigns to the Institute of Technology (Banaras Hindu University) Varanasi all rights under copyright that may exist in and for the above thesis submitted for the award of the *“DOCTOR OF PHILOSOPHY”* .

Date: 26 December 2022

Place: IIT (BHU), Varanasi



Signature of the Student

(Tushar Sarkar)

Note: However, the author may reproduce or authorize others to reproduce material extracted verbatim from the thesis or derivative of the thesis for the author's personal use provided that the source and the Institute's copyright notice are indicated.

ACKNOWLEDGMENTS

“गुरु ब्रह्मा गुरु विष्णु, गुरु देवो महेश्वरा गुरु साक्षात् परब्रह्म, तस्मै श्री गुरुवे नमः”

No one who achieves success does so without acknowledging the help of others. The wise and confident acknowledge this help with gratitude.

Alfred North Whitehead

Foremost, I express my deep sense of gratitude to my research supervisor Dr. Rakesh Kumar Singh for his excellent guidance, motivation, and constant encouragement during my entire research work. The completion of this research work is indeed an outcome of his support, valuable ideas, and suggestions. The insightful discussion with him always provided me with great enthusiasm. I express my gratitude to the Head of the Department for providing me required facilities. I am extremely thankful to my RPEC members Dr. Imtiyaz Ahmad and Dr. Sunil Kumar Singh for their invaluable inspiration, kind support, and numerous insightful suggestions during the entire course of this research. I am also grateful to Dr. Rajeev Singh, IIT(BHU), Dr. Maruti M. Brundavanam, IIT (Kharagpur), and Dr. Nandan S. Bisht, Kumaun University (Nainital), for their valuable support in the form of insightful discussions and lab facility.

I use this opportunity to express my gratefulness to all the faculty members of the Department of Physics for their kind encouragement and motivation during my research period. I am also thankful to the entire non-teaching staff of the Department of Physics.

I am also grateful to Reajmina Parvin, IIT (Kharagpur), and Vipin Tiwari, Kumaun University (Nainital), for their unconditional support and help during my collaborative research work. I wish to thank my lab companions and friends Manisha, Sourav, Akanksha, Sarita, and all lab members of “Laboratory of Information Photonics and Optical Metrology, Department of Physics, IIT (BHU)” for providing me with a conducive environment to carry out my research work.

I would also like to express my sincere appreciation to my colleagues and friends Kuldeep Shrivastava, and all research scholars of the department for their lively friendship and continuous support at all stages of my research.

I feel short of words to express my appreciation, gratitude, and indebtedness to my dearest friend Manisha Sarkar and my family members, my father Shri Naryan Sarkar, and mother Smt. Baby Sarkar, Sister Puja & Pallavi, and their whole family for their

unbounded love, blessings, encouragement, and support during my entire academics. Many others that have been involved also deserve recognition. It is, however, not possible to list them all here. Their support in this effort is, however, greatly appreciated. Finally, I am grateful to the Almighty for giving me the patience to make this endeavor a success.

Sincerely
(Tushar Sarkar)

This thesis is dedicated to all those who have chosen excellence over success.

Confidence and doubt are like two bulls in a car—either confidence is going to stay or your doubts or insecurities are going to stay, but there is not room for both to remain.

Keith Johnson

Success is no accident. It is hard work, perseverance, learning, studying, sacrifice, and most of all, love of what you are doing or learning to do.

Pele

*Welcome
To
World of Optics*

*Dedicated
To
My Beloved
Family*

“No amount of money or success can take the place of time spent with your family”

TABLE OF CONTENTS

CERTIFICATE	ii
DECLARATION BY THE CANDIDATE	iii
COPYRIGHT TRANSFER CERTIFICATE	iv
ACKNOWLEDGMENTS	v
TABLE OF CONTENTS	x
LIST OF FIGURES	xiii
Chapter 1	22
Introduction.....	22
1.1 Optical information processing.....	24
1.2 Delivering optical information.....	27
1.2.1 Plane-wave	27
1.2.2 Helical beam	28
1.3 Helical modes for the delivery of optical information.....	29
1.4 Origin of helical beam	31
1.5 Generation of a helical beam	34
1.5.1 Spiral phase plate	34
1.5.2 Diffractive optical elements	35
1.5.3 Spatial light modulator (SLM).....	36
1.6 Detection of helical beam	37
1.6.1 Interferometric techniques	37
1.6.2 Diffraction techniques.....	38
1.6.3 Deep learning	40
1.7 Applications of helical beam	41
1.7.1 Optical communication.....	41
1.7.2 High-resolution imaging	43
1.8 Optical information using holography	44
1.9 Optical information delivery through randomness	47
1.9.1 Optical phase conjugation.....	49
1.9.2 Optical memory effect	50
1.9.3 Correlation optics approach	51
1.9.3.1 The complex coherence function	51
1.9.3.2 Intensity correlation	53
1.9.3.3 Characterization of vectorial random field	55
1.9.3.4 Coherence polarization matrix	58
1.9.3.5 HBT for polarized light.....	59
1.9.3.6 Polarization correlation.....	61
1.10. Delivery and recovery of 3D optical information with coherence holography	64
Chapter 2	68

New experimental designs and techniques to recover OAM modes from randomness	68
2.1 Introduction.....	70
2.2 Stokes fluctuations correlation.....	72
2.3 Higher order Stokes parameters correlation	78
2.3.1 Theoretical basis	79
2.3.2 Simulation results.....	81
2.3.3 Experiment and results discussions	83
2.3.4 Mode analysis	86
2.4 Digital phase-shifting with Stokes correlation.....	88
2.4.1 Theoretical model	90
2.4.2 Simulation results.....	92
2.4.3 Experiment and results discussions	93
2.4.4 OAM mode characterization.....	97
2.5 Conclusion	98
Chapter 3	100
Recovering mixtures of OAM modes from randomness	100
3.1 Introduction.....	102
3.2 Higher-order polarization correlation	105
3.3 Recovering a mixture of OAM modes and fractional charge from randomness	106
3.3.1 Theory	107
3.3.2 Simulation results.....	111
3.3.3 Experiment and results discussions	113
3.3.4 OAM modes decomposition and their need.....	117
3.4 Measuring OAM modes by a three-step phase-shifting in the polarization correlations. 120	
3.4.1 Theoretical framework.....	121
3.4.2 Simulation results.....	123
3.4.3 Experiment and results discussions	125
3.4.4 OAM spectrum analysis.....	128
3.5 Conclusion	130
Chapter 4	132
Estimation of the topological charge of the helical beam from the random light.....	132
4.1 Introduction.....	134
4.2 Theoretical basis	136
4.3 Simulation results.....	141
4.4 Experiment.....	142
4.5 Results and discussions.....	144
4.6 Conclusion	146

Chapter 5	148
Correlation holography with unpolarized light.....	148
5.1 Introduction.....	150
5.2 Stokes correlation of randomly polarized light.....	153
5.3 Higher-order Stokes correlation holography	155
5.3.1 Theoretical basis	155
5.3.2 Simulation results.....	159
5.3.3 Experiment and results discussions	161
5.4 On-axis phase-shifting correlation holography.....	165
5.4.1 Theoretical background	166
5.4.2 Simulation results.....	168
5.4.3 Experiment and results discussions	170
5.5 Conclusion	174
Chapter 6	176
Conclusion	176
6.1 Summary	178
6.2 Future Work	182
Bibliography	184
List of Publications	200

LIST OF FIGURES

Fig. 1.1 Schematic for optical information processing	25
Fig. 1.2 (a) Shows the spectrum of the letter “IIT BHU”, (b) represents the original image.....	26
Fig. 1.3 Spatial filtering of the letter “IIT BHU” in the focal plane with the low pass filter (a) low pass filter at the focal plane, (b) representing the corresponding image.	27
Fig. 1.4 Shows a plane wave.....	28
Fig. 1.5 (a) Shows OAM beams, (b) indicates LG beams.	29
Fig. 1.6 Schematic representation of physical dimensions of photons (frequency/wavelength, time, complex amplitude, polarization, spatial structure) and orthogonal states (multiple wavelengths, time slots, constellation points in the complex plane, X- and Y-polarizations, phase vortices) (Wang, 2016).....	30
Fig. 1.7 Orbital angular momentum (OAM)-multiplexed free-space optical airborne and satellite communications (Willner, 2021).....	31
Fig. 1.8 Helical beams of different TC with their phase and intensity profile.	34
Fig. 1.9 Schematic of the generation of a helical beam with SPP.	35
Fig. 1.10 Represents the phase hologram with $l=3$. (a) shows spiral phase hologram, (b) indicates l -fold forked hologram, (c) denotes binarized l -fold forked grating.	36
Fig. 1.11 Generation of vortex beam using SLM.	37
Fig. 1.12 Mach Zehnder configuration for measuring the OAM of the vortex beam. BS: Beam splitter, M: mirror, SPP: spiral phase plate.....	38
Fig. 1.13 Diffraction pattern of different helical beams at the far field using triangular aperture (Araujo, 2011).....	39
Fig. 1.14 The learning model for helical beam detection (Li, 2008).	40
Fig. 1.15 Schematic of optical vortex modulation and multiplexing (Wang, 2016).	42
Fig. 1.16 (a) Multiple OAM beams are coaxially transmitted through free space. (b) Each orthogonal OAM beam carries an independent data stream (Willner, 2021).	42
Fig. 1.17 (a) Represents a sketch of STED, (b) denotes effective PSF (Hirsemenzel, 2013).	43
Fig. 1.18 Basic geometries for holography.....	45
Fig. 1.19 Generation of the speckle pattern.	47
Fig. 1.20 (a) Co-axial propagation of OAM modes for delivery of optical information (Gong, 2019), (b) imaging of hidden object behind the random scattering media.	48
Fig. 1.21 Schematic of OPC.	49
Fig. 1.22 Schematic of the memory effect: an incident-tilted source results in the shift of the speckle pattern in the observation plane.	50
Fig. 1.23 Schematic for the scattering of coherent light from a random scattering media and generation of the randomly scattered field at the observation plane.....	53

Fig. 1.24 Schematic diagram for intensity correlation measurement.	54
Fig. 1.25 Sketch for generation of polarization speckle. Polarization state distribution in part of the speckle is highlighted on the right-hand side.	57
Fig. 1.26 (a) Snapshot of the fluctuating random field, (b) dynamics of polarization change in a single random pattern (at a frozen time t) is represented at the Poincare sphere. The SOPs in the random field is varying from point A to B. (Singh, 2014).	58
Fig. 1.27 Schematic diagram of intensity correlation of vector field.	60
Fig. 1.28 Schematic diagram for the polarization-resolved HBT experiment.	61
Fig. 1.29 (a) Reconstruction in conventional holography with coherent illumination, (b) reconstruction in coherence holography with random light.	65
Fig. 1.30 (a), (b) Denote schematic for temporal and spatial averaging operations respectively. RGG: rotating ground glass, SGG: static ground glass.	66
Fig. 2.1 Generation of the speckle pattern.	73
Fig. 2.2 Conceptual representation of the proposed technique with OAM mode and polarization guiding. Generation of random electromagnetic fields by orthogonally polarized light. x and y polarization components represent helical and non-helical wavefronts of the incident light. A CCD records intensity speckle patterns at the observation plane. These speckle patterns are used to determine four SPs and subsequently, higher-order SPs correlations provide the structure of the incident helical wavefront.	79
Fig. 2.3 Simulation results; (a-c) amplitude distribution of complex polarization correlation function for three different cases, (d-f) are the corresponding phase distribution.	82
Fig. 2.4 An experimental setup to detect twisted wavefront from the randomly scattered intensity. NDF: neutral density filter, HWP: half-wave plate, BS: beam splitter, SLM: spatial light modulator, GG: ground glass, QWP: quarter-wave plate, LP: linear polarizer, CCD: charge-coupled device. The dumped beam is not used in the experiment.	84
Fig. 2.5 Experimentally measured SPs.	85
Fig. 2.6 Simulation results; (a-c) amplitude distribution of complex polarization correlation function for three different cases, (d-f) are the corresponding phase distribution.	86
Fig. 2.7 Panels (a-c), (d-f) represent simulation and experimental results for the OAM distribution for three different OAM modes $l = 1, 2, 3$	88
Fig. 2.8 Schematic for conventional phase-shifting technique.	88
Fig. 2.9 Conceptual sketch of the four-phase shifting technique for coherence wave.	90
Fig. 2.10 Indicate helical phase distribution for two different cases respectively.	93
Fig. 2.11 Schematic of the experimental set-up of the proposed technique. He-Ne Laser, NDF is a neutral density filter, HWP is a half-wave plate, BS is a beam splitter, SLM is a spatial light modulator, GG is ground glass, LP is a linear polarizer, CCD is a charge-coupled device.	93

Fig. 2.12 Experimentally measured SPs (S_0, S_1, S_2) of the phase profile of the vortex beam for phase shifts of $0, \pi/2, \pi$, and $3\pi/2$ and (m-p) represent the corresponding real part.	95
Fig. 2. 13 Experimentally recovered helical wavefront for two different cases respectively.	96
Fig. 2.14 Panels (a, b), (c, d) indicate simulation and experimental results for the OAM distribution for two different OAM modes $l = 1, 2$	98
Fig. 3.1 (a) Slit and its spatial frequency, (b) Azimuthal target and its OAM spectrum.	102
Fig. 3.2 Schematic representation of $f - f$ geometry and the formation of speckle at the Fourier transform plane.....	109
Fig. 3.3 Simulation results for free space; (a-c) represent amplitude distribution for three different cases $l=-0.5, 0.5, 1.5$, (d-f) are the corresponding phase distribution. The dark lines in the amplitude distribution are highlighted in the inset.	112
Fig. 3.4 Simulation results for random media; (a-c) represent amplitude distribution of CPCF for three different cases $l=-0.5, 0.5, 1.5$, (d-f) are the corresponding phase distribution. The dark lines in the amplitude distribution are highlighted in the inset.	113
Fig. 3.5 Sketch of the experimental set-up of the proposed technique. He-Ne Laser, NDF: Neutral density filter, HWP: Half-Wave plate, BS: Beam splitter, SLM: Spatial light modulator, GG: Ground glass, L: Lens, QWP: Quarter-Wave plate, LP: Linear polarizer, CCD: Charge-coupled device.	114
Fig. 3.6 Represents experimentally measured SPs (a) S_0 (b) S_1 (c) S_2 and (d) S_3	115
Fig. 3.7 Experiment results for random media; (a-c) represent amplitude distribution of CPCF for three different cases $l=-0.5, 0.5, 1.5$, (d-f) are the corresponding phase distribution. The dark lines in the amplitude distribution are highlighted in the inset.	116
Fig. 3.8 Panels (a-c), (d-f) represent simulation and experimental results of the scattering media for the OAM distribution for three different OAM modes with $l=-0.5, 0.5$, and 1.5	119
Fig. 3.9 Schematic representation of the three-step phase-shifting technique with SPs correlations.....	121
Fig. 3.10 Simulation results: (a-b), (c-d) show amplitude distributions of the CPCF for IVB and FOV with TC values $l=1, 2$, and $n=-0.5, 1.5$, respectively. (e-f), (g-h) are the corresponding phase distributions.....	124
Fig. 3.11 Experimental sketch of the developed technique. He-Ne Laser, BS: beam splitter, HWP: half-wave plate, SLM: spatial light modulator, GG: ground glass, LP: linear polarizer, CMOS: complementary metal-oxide-semiconductor.	126
Fig. 3.12 Experimentally measured SPs of the scattered field. (a-c), (d-f), and (g-i) depict the first three SPs (S_0, S_1, S_2) for VB with $l=1$ with phase shifts of $0, 2\pi/3$, and $4\pi/3$, respectively.	127
Fig. 3.13 Experimental results: (a-b), (c-d) show amplitude distributions of CPCF for VB and FOV with TC values $l=1, 2$, and $n=-0.5, 1.5$, respectively. (e-f), (g-h) are the corresponding phase distributions.....	128

Fig. 3.14 OAM power spectrum: The blue panels in Figs. (a, b), (c, d) show OAM simulation results for IVB and FOV with TC values $l=1, 2$, and $n=-0.5, 1.5$. Red panels are the corresponding experimental results..... 129

Fig. 4.1 Schematic representation of the creation of the random electromagnetic field by orthogonally polarized incident light fields. 138

Fig. 4.2 (a-c) Represent simulation results for the distribution of correlation function for vortex with $m=1, 2, 3$ respectively. 142

Fig. 4.3 An experimental setup to estimate the TC of the vortex beam from the speckle pattern. NDF: neutral density filter, HWP: half-wave plate, BS: beam splitter, SLM: spatial light modulator, GG: ground glass, QWP: quarter-wave plate, LP: linear polarizer, CCD: charge-coupled device. The dumped beam is not used in the experiment. 143

Fig. 4.4 Denotes experimentally measured SPs from the recorded intensity speckle patterns. (a, b), (c, d), (e, f) show SPs of the vortex with $l=1, 2, 3$ respectively. 145

Fig. 4.5 (a-c) Represent experimental results for the distribution of correlation function for vortex with $m=1, 2, 3$ respectively..... 145

Fig. 5.1 Schematic representation of recoding and reconstruction of the FTH hologram. (a) denotes the recording of the FTH hologram, L represents the lens of focal length f . (b) shows the incoherent reconstruction of the FTH by random light at a distance $z=f$ 157

Fig. 5.2 Simulation results: (a, b) represent amplitude distribution of the vortex with $l=1$ and number 2. (c, d) are the corresponding phase distribution. The magnified images of the amplitude and phase distribution of the vortex are shown in the inset of Figs. 5.2 (a) and 5.2 (c) respectively. Pixel numbers are given on both axes. 160

Fig. 5.3 Experimental implementation of the proposed technique. Laser: Solid random polarized diode laser, MO: Microscope objectives, P: Pinhole, L: lens, PBS: Polarizing beam splitter, M: Mirror, SLM: Spatial light modulator, GG1, GG2: Ground glasses, BS1, BS2: Beam splitters, QWP: Quarter wave plate, LP1, LP2: Linear polarizers, CCD: Charge-coupled device..... 162

Fig. 5.4 Represent experimentally measured SPs from the captured intensity patterns. (a,b) represent SPs of the vortex with $l=1$ and (c, d) show SPs of number 2. Pixel numbers are given on both axes..... 163

Fig. 5.5 Experimental results: (a, b) represent amplitude distribution of the vortex with $l=1$ and number 2. (c, d) are the corresponding phase distribution. The magnified images of the amplitude and phase distribution of the vortex are shown in the inset of Figs. 5.5(a) and 5.5(c) respectively. Pixel numbers are given on both axes. 164

Fig. 5.6 Schematic representation: Reconstruction of the FH with un-polarized light from the randomness..... 166

Fig. 5.7 (a, b) show the amplitude distribution of the vortex beam with TC $l=1, 3$, and (d, e) are the corresponding phase profile respectively. (c) indicates the amplitude profile of the Laguerre-Gaussian beam with mode $l=1, p=1$, (f) denotes the corresponding phase profile respectively..... 170

Fig. 5.8 Schematic of the optical set-up. He-Ne Laser, MO: microscopic objective, P: pinhole, L_1, L_2, L_3 : lenses, PBS: polarizing beam splitter, HWP_1, HWP_2 : half-wave plates, M: mirror, SLM: spatial light modulator, GG ground glass, QWP: quarter-wave plate, LP:

linear polarizer, CCD: charge-coupled device. The propagation of the object beam (red) and reference beam (blue) from L_3 to GG is shown in the inset..... 171

Fig. 5.9 (a-d) Represent experimentally measured S_2 for phase shifts of 0 , $\pi/2$, π , and $3\pi/2$ of the Laguerre-Gaussian mode with $l=1$, $p=1$. (e-h) are the corresponding real part of the CPCF..... 173

Fig. 5.10 (a, b) show the amplitude distribution of the vortex beam with TC $l=1, 3$, (d, e) are the corresponding phase profile respectively. (c) indicates the amplitude profile of the Laguerre-Gaussian beam with mode $l=1$, $p=1$, and (f) denotes the corresponding phase profile respectively..... 173

PREFACE

The objective of the research presented in the thesis is to investigate issues and challenges of the random scattering of light and present our new results. The thesis reports new experimental schemes with helical modes of light and polarization to faithfully deliver and recover the information through a random scattering media. Polarization guiding and encoding information into one of the orthogonal polarization modes of the light work as a pilot-assisted strategy to deliver coherent light through a random scattering medium and consequently see through the scatterer by polarization correlation.

The research work presented in this thesis has been divided into **six** chapters.

Chapter 1 presents an introduction on the information optics and delivering coherent optical signals through the free space and scattering media. This chapter starts a discussion on the coherent optical signals, wavefront shaping, and mode composition of the light in information optics. Apart from using the conventional method to examine the plane wave composition in the optics, we discuss and give special emphasis to the helical modes of light in the information optics. The role of helical modes and holography in the processing of optical information is also discussed. However, inhomogeneity of refractive index distributions in the scattering path scrambles the optical signal without any direct resemblance to the desired information and hence makes conventional optical methods nearly redundant. Intensive research efforts have been made to address this fundamental, yet practical, problem, and many different techniques have been put forward. This chapter covers the challenges of faithful delivery of optical signals through random light, different techniques, limitations, and the role of coherence in optics through randomness particularly on looking through randomness.

In **Chapter 2**, we propose two different techniques to quantitatively determine the helical mode of the beam scrambled by a random scattering medium. In the first technique, the SPs of the randomly scattered field is exploited to recover complex polarization correlation function (CPCF) which adduces the information of the helical beam. The two-point correlation of the SPs provides a 4-by-4 matrix with sixteen elements. Out of these sixteen elements, only four elements of the matrix are used to obtain real and imaginary parts of the CPCF. This technique requires six measurements to evaluate the SPs from the randomly scattered fields using a polarizer and quarter-wave plate (QWP) in the experiment. The use of a QWP in the Stokes polarimetry demands proper calibration in power to avoid unnecessary influence on the state of polarization (SOP) mapping owing to the absorption of light by the QWP. Therefore, the second technique is built on the principle of using limited SPs without the QWP and quantitatively retrieves the helical mode from the random light in a lensless configuration. The correlation of the first three SPs of the random light combined with digital phase shifting for the recovery of helical mode. The correlation of the first three SPs forms a 3-by-3 matrix that contains nine elements. Out of these nine elements, only two elements of the matrix along with four phase-shifting are applied to recover the helical mode from the random light. This helps to design a highly stable experimental setup. Detailed theoretical frameworks, numerical simulations, and experimental results of these techniques are discussed.

Chapter 3 presents two different techniques for the recovery and sorting of the composition of helical modes propagating through the random scattering media. The first technique uses the all SPs of the scattered polarized field to evaluate the higher-order polarization correlation and subsequently the CPCF. The complex amplitude of the composition of the helical modes is extracted from the random light using the CPCF. In comparison to the previous chapter, here we demonstrate the recovery of the composition

of helical modes and their weightage in different optical signals. The two-point correlation of the Stokes fluctuations assists to design a highly stable non-interferometric configuration to recover compositions of helical modes from the random light. Another experimental set-up free from the QWP is also built to design a new lensless non-interferometric experimental geometry for recovery of the composition of OAM modes from the random light. This technique employs the limited SPs which are measured by only a linear polarizer. The correlation of the limited SPs of the random light along with three-step phase shifting is used to evaluate the complex Fourier coefficient (CFC). The CFC helps to extract the complex amplitude of the compositions of helical modes. The orthogonal projection method is further used to sort the different integer OAM modes in terms of the OAM power spectrum from the recovered complex amplitude. The detailed theoretical models, numerical simulations, and experimental results of these techniques are explained.

Chapter 4 describes a new approach to estimating the helical mode of the beam from the non-imaged randomly scattered pattern. SPs of the random light are used and higher-order correlations between SPs fluctuations are evaluated in this approach. This provides a 4-by-4 correlation matrix that contains sixteen elements. Out of these sixteen elements, only one element is considered to build a theoretical basis and subsequently applied for the estimation of the helical mode of the incident optical signal. We design a highly stable experimental geometry in a coaxial propagation of two orthogonal polarization states of the light to estimate the helical mode from the speckle pattern. The topological charge of the helical beam is estimated by counting the number of petals in the correlation function of the Stokes parameter. A detailed theoretical model, numerical simulation of the experimental situation with Stokes correlation, and experimental results are presented to test and confirm our approach.

Chapter 5 presents two different correlation holography approaches with randomly polarized light for 3D optical information recovery. Here, we demonstrate two different strategies on how to use depolarization for the reconstruction of the correlation holography. In the first approach, the higher-order polarization correlation of the randomly polarized light is exploited to design an in-line correlation holography technique through the random scattering media. Only two SPs of the randomly polarized light are employed to evaluate the CPCF and this recovers the complex amplitude using higher-order polarization correlations. This is a new method for lensless and in-line complex field reconstruction in correlation holography. In the second approach, only a single SP of randomly polarized light is combined with digital phase shifting to build a robust and compact lensless in-line holography reconstruction method with the random light. The higher-order polarization correlation is used to obtain the real part of the CPCF from the SP of the randomly polarized light. The four-phase shifting method is combined with real parts of the CPCF to appraise the CFC and consequently in the reconstruction of the hologram. The detailed theoretical analysis, numerical simulations, and experimental tests of these two techniques are described in the chapter.

The conclusions of the overall study have been summarized in the last **chapter 6**. We discuss the role of polarization correlation in the recovery of OAM modes and in unconventional holography techniques to deliver and recover optical information with randomness. This Chapter also comprises further future research plans on this topic, particularly on encoding, non-line of sight (NLOS), and underwater imaging.